Article:

Ward, JA and Grindrod, P (2014) Aperiodic dynamics in a deterministic adaptive network model of attitude formation in social groups. Physica D: Nonlinear Phenomena, 282. pp. 27-33. ISSN: 0167-2789

https://doi.org/10.1016/j.physd.2014.05.006

Aperiodic dynamics in a deterministic adaptive network model of attitude formation in social groups

Jonathan A. Ward

School of Mathematics, University of Leeds, Leeds, LS2 9JT UK

Peter Grindrod

Mathematical Institute, University of Oxford, Oxford, OX2 6GG UK

Abstract

Adaptive network models, in which node states and network topology coevolve, arise naturally in models of social dynamics that incorporate homophily and social influence. Homophily relates the similarity between pairs of nodes' states to their network coupling strength, whilst social influence causes coupled nodes' states to convergence. In this paper we propose a *deterministic* adaptive network model of attitude formation in social groups that includes these effects, and in which the attitudinal dynamics are represented by an activator-inhibitor process. We illustrate that consensus, corresponding to all nodes adopting the same attitudinal state and being fully connected, may destabilise via Turing instability, giving rise to aperiodic dynamics with sensitive dependence on initial conditions. These aperiodic dynamics correspond to the formation and dissolution of sub-groups that adopt contrasting attitudes. We discuss our findings in the context of cultural polarisation phenomena.

Email address: `j.a.ward@leeds.ac.uk` (Jonathan A. Ward)

Preprint submitted to Physica D *April 24, 2014*

Keywords: , Adaptive networks, social dynamics, dynamical systems, social networks, activator-inhibitor, chaos, social influence, homophily
37N99, 97M70, 91D30

1. Introduction

In an adaptive network, the evolution of the states of nodes in the network coevolve with the network topology [1]. Adaptive network models have been proposed to describe a range of phenomena, including synchronisation [2, 3, 4], epidemics [5, 6], cooperation [7, 8, 9] and opinion dynamics [10, 11, 12, 13, 14, 15, 16]. See Gross and Blasius [1] for a review. As with most complex systems, the usual paradigm is to describe the model dynamics via a stochastic process. In this paper we take an alternative approach, using an adaptive network described by a *deterministic* continuous-time dynamical system, which we use as a model for attitude formation in social groups. Earlier studies of deterministic adaptive network models have focussed on synchronisation in systems of coupled oscillators [17, 18], although discrete-time models of opinion dynamics have also been proposed [19, 20]. Part of our goal is to illustrate how techniques from nonlinear dynamics may be used to study adaptive networks in a way that compliments the typical statistical physics approach [21].

In this paper we consider a model of attitude formation in social groups, where the attitude of each node, or agent, in the system is described by a vector of states and the interaction patterns between agents are governed by an evolving weighted network. Our model incorporates two key behavioural mechanisms:

1. **Social influence.** This reflects the fact that people tend to modify their behaviour and attitudes in response to the opinions of others [22, 23, 24, 25, 26]. We model social influence via diffusion: agents adjust their state according to a weighted sum (dictated by the evolving network) of the differences between their state and the states of their neighbours.

2. **Homophily.** This relates the similarity of individuals' states to their frequency and strength of interaction [27]. Thus in our model, homophily drives the evolution of the weighted 'social' network.

A precise formulation of our model is given in Section 2. Social influence and homophily underpin models of social dynamics [21], which cover a wide range of sociological phenomena, including the diffusion of innovations [28, 29, 30, 31, 32], complex contagions [33, 34, 35, 36], collective action [37, 38, 39], opinion dynamics [19, 20, 40, 10, 11, 13, 15, 41, 16], the emergence of social norms [42, 43, 44], group stability [45], social differentiation [46] and, of particular relevance here, cultural dissemination [47, 12, 48].

Combining the effects of social influence and homophily naturally gives rise to an adaptive network, since social influence causes the states of agents that are strongly connected to become more similar, while homophily strengthens connections between agents whose states are already similar[1]. It is surprising then that the feedback between homophily and social influence does not necessarily lead to consensus or 'monoculture' [47], where all nodes have

[1]Note, however, that differentiating between the effects of homophily and social influence in observational settings may be very difficult [49, 50].

identical states and are fully connected. Instead, cultural polarisation may occur: equilibria in which groups of nodes have identical states, but several different groups exist. Typically, cultural polarisation arises from the creation of 'structural holes' [51], which at its extreme leads to fragmentation of the network [15, 16]. However, cultural polarisation is not necessarily stable when there is 'cultural drift', i.e. small, random perturbations or noise, which drive the system towards monoculture [52]. Since diversity and even polarisation of opinions are observed in society [47, 48], there have been a number of attempts to develop models with polarised states that are stable in the presence cultural drift [12, 48], but this is still an open problem [21].

In this paper, we investigate whether a general class of activator-inhibitor processes on an adaptive network can give rise to polarisation of attitudes. While the resulting dynamics illustrate that such systems are interesting in their own right, they are also perhaps a natural choice in the context of *sub-conscious* attitude formation. Neuropsychological evidence suggests that the *activation* of emotional responses and the *regulation* of inhibitions are associated with different parts of the brain [53]. This has led psychologists to develop theories in which various personality traits (such as extroversion, impulsivity, neuroticism and anxiety) form an independent set of dimensions along which different types of behaviour may be excited or regulated [54, 55, 56]. There is also substantial evidence that such automated and sub-conscious processes play an important role in evaluations and judgements [57]. Thus while it may be extremely difficult to perform empirical measurements on which models of sub-conscious attitude formation may be based, such processes almost certainly influence what we perceive to be conscious decision making.

One of the benefits of our dynamical systems formulation is that we are able to analyse the stability of the consensus equilibrium, and in Section 2 we show that Turing instability can arise. Furthermore, in Section 3 we illustrate, via numerical simulations, that the tension between Turing instability and the coevolution of the social network and attitudinal states gives rise to aperiodic dynamics that have a sensitive dependence on initial conditions. These dynamics correspond to the formation and dissolution of sub-groups that adopt distinct, non-equilibrium, attitudinal states. In Section 4 we discuss the transient patterns we observe in the context of cultural polarisation observed in other models.

2. A deterministic model of attitude formation

In this section we give a precise description of our adaptive network model of sub-conscious attitude formation in social groups. This model consists of two sets of coupled ordinary differential equations, one to describe the dynamics of agents' attitudinal states and the other to describe the evolution of the coupling strengths between nodes.

Consider a population of N identical individuals (nodes/agents/actors), each described by a set of M real attitude state variables that are continuous functions of time t. Let $\mathbf{x}_i(t) \in \mathbb{R}^M$ denote the ith individual's attitudinal state. In the absence of any influence or communication between agents we assume that each individual's state obeys an autonomous rate equation of the form

$$\dot{\mathbf{x}}_i = \mathbf{f}(\mathbf{x}_i), \quad i = 1, ..., N, \tag{1}$$

where $\mathbf{f}$ is a given smooth field over $\mathbb{R}^M$, such that $\mathbf{f}(\mathbf{x}^*) = 0$ for some $\mathbf{x}^*$. Thus (1) has a uniform population equilibrium $\mathbf{x}_i = \mathbf{x}^*$, for $i = 1, ..., N$, which we shall assume is locally asymptotically stable. As discussed in the introduction, we shall more specifically assume that (1) is drawn from a class of activator-inhibitor systems [58, 59, 60].

Now suppose that the individuals are connected up by a dynamically evolving weighted network. Let $A(t)$ denote the $N \times N$ weighted adjacency matrix for this network at time t, with the ijth term, $A_{ij}(t)$, representing the instantaneous weight (frequency and/or tie strength) of the mutual influence between individual i and individual j at time t. Throughout we assert that $A(t)$ is symmetric, contains values bounded in [0,1] and has a zero diagonal (no self influence). We extend (1) and adopt a first order model for the coupled system:

$$\dot{\mathbf{x}}_i = \mathbf{f}(\mathbf{x}_i) + D \sum_{j=1}^{N} (\mathbf{x}_j - \mathbf{x}_i)\, A_{ij}(t), \quad i = 1, ..., N. \tag{2}$$

Here D is a real, diagonal and non-negative matrix containing the maximal transmission coefficients (diffusion rates) for the corresponding attitudinal variables between neighbours. Thus some of the attitude variables may be more easily or readily transmitted, and are therefore influenced to a greater extent by (while simultaneously being more influential to) those of neighbours. Note that $\mathbf{x}_i = \mathbf{x}^*$, for $i = 1, ..., N$, is also a uniform population equilibrium of the augmented system.

Let $\mathbf{X}(t)$ denote the $M \times N$ matrix with ith column given by $\mathbf{x}_i(t)$, and $\mathbf{F}(\mathbf{X})$ be the $M \times N$ matrix with ith column given by $\mathbf{f}(\mathbf{x}_i(t))$. Then (2) may be written as

$$\dot{\mathbf{X}} = \mathbf{F}(\mathbf{X}) - D\mathbf{X}\Delta. \tag{3}$$

Here $\Delta(t)$ denotes the weighted graph Laplacian for $A(t)$, given by $\Delta(t) = \text{diag}(\mathbf{k}(t)) - A(t)$, where $\mathbf{k}(t) \in \mathbb{R}^N$ is a vector containing the degrees of the vertices ($k_i(t) = \sum_{j=1}^{N} A_{ij}(t)$). Equation (3) has a rest point at $\mathbf{X} = \mathbf{X}^*$, where the ith column of $\mathbf{X}^*$ is given by $\mathbf{x}^*$ for all $i = 1, ..., N$.

To close the system, consider the evolution equation for the ijth edge, $A_{ij}(t)$, given by

$$\dot{A}_{ij} = \alpha A_{ij}(1 - A_{ij})(\varepsilon - \phi(|\mathbf{x}_i - \mathbf{x}_j|)). \tag{4}$$

Here $\alpha > 0$ is a rate parameter; $\varepsilon > 0$ is a homophily scale parameter; $|\cdot|$ is an appropriate norm or semi-norm; and $\phi : \mathbb{R} \to \mathbb{R}$ is a real function that incorporates homophily effects. We assume that $\phi(|\mathbf{x}_i - \mathbf{x}_j|) \geq 0$ and that ϕ is monotonically increasing with $\phi(0) = 0$. Note that the sign of the differences held in $\varepsilon - \phi(|\mathbf{x}_i - \mathbf{x}_j|)$ controls the growth or decay of the corresponding coupling strengths. The matrix $A(t)$ is symmetric, so in practice we need only calculate the super-diagonal terms. The nonlinear "logistic growth"-like term implies that the weights remain in [0,1], while we refer to the term $\varepsilon - \phi(|\mathbf{x}_i - \mathbf{x}_j|)$ as the *switch* term.

2.1. Stability analysis

By construction, there are equilibria at $\mathbf{X} = \mathbf{X}^*$ with either $A = 0$ or $A = \mathbf{1}$, where $\mathbf{1}$ denotes the adjacency matrix of the fully weighted connected graph (with all off-diagonal elements equal to one and all diagonal elements equal to zero). To understand their stability, let us assume that $\alpha \to 0$ so that $A(t)$ evolves very slowly. We may then consider the stability of the uniform population, $\mathbf{X}^*$, under the fast dynamic (3) for any fixed network A. Assuming that A is constant, writing $\mathbf{X}(t) = \mathbf{X}^* + \tilde{\mathbf{X}}(t)$ and Linearising (3) about $\mathbf{X}^*$, we obtain

$$\dot{\tilde{\mathbf{X}}} = \mathbf{df}(\mathbf{x}^*)\tilde{\mathbf{X}} - D\tilde{\mathbf{X}}\Delta. \tag{5}$$

Here $\mathbf{df}(\mathbf{x}^*)$ is an $M \times M$ matrix given by the linearisation of $\mathbf{f}(\mathbf{x})$ at $\mathbf{x}^*$. Letting $(\lambda_i, \mathbf{w}_i) \in [0, \infty) \times \mathbb{R}^N,\ i = 1, ..., N$, be the eigen-pairs of Δ, then we may decompose uniquely [61]:

$$\tilde{\mathbf{X}}(t) = \sum_{i=1}^{N} \mathbf{u}_i(t)\mathbf{w}_i^T,$$

where each $\mathbf{u}_i(t) \in \mathbb{R}^M$. The stability analysis of (5) is now trivial since decomposition yields

$$\dot{\mathbf{u}}_i = (\mathbf{df}(\mathbf{x}^*) - D\lambda_i)\mathbf{u}_i.$$

Thus the uniform equilibrium, $\mathbf{X}^*$, is asymptotically stable if and only if all N matrices, $(\mathbf{df}(\mathbf{x}^*) - D\lambda_i)$, are simultaneously stability matrices; and conversely is unstable in the ith mode of the graph Laplacian if $(\mathbf{df}(\mathbf{x}^*) - D\lambda_i)$ has an eigenvalue with positive real part.

Consider the spectrum of $(\mathbf{df}(\mathbf{x}^*) - D\lambda)$ as a function of λ. If λ is small then this is dominated by the stability of the autonomous system, $\mathbf{df}(\mathbf{x}^*)$, which we assumed to be stable. If λ is large then this is again a stability matrix, since D is positive definite. The situation, dependent on some collusion between choices of D and $\mathbf{df}(\mathbf{x}^*)$, where there is a *window of instability* for an intermediate range of λ, is know as a Turing instability. Turing instabilities occur in a number of mathematical applications and are tied to the use of activator-inhibitor systems (in the state space equations, such as (1) here), where inhibitions diffuse faster than activational variables.

Now we can see the possible tension between homophily and Turing instability in the attitude dynamics when the timescale of the evolving network, α, is comparable to the changes in agents' states. There are two distinct types of dynamical behaviour at work. In one case, $\Delta(t)$ has presently no eigenvalues within the window of instability and each individual's states $\mathbf{x}_i(t)$ approach the mutual equilibrium, $\mathbf{x}^*$; consequently all switch terms become positive and the edge weights all grow towards unity, i.e. the fully weighted clique. In the alternative case, unstable eigen-modes cause the individual states to diverge from $\mathbf{x}^*$, and subsequently some of the corresponding switch terms become negative, causing those edges to begin losing weight and hence partitioning the network.

The eigenvalues of the Laplacian for the fully weighed clique, $A = \mathbf{1}$, are at zero (simple) and at N (with multiplicity $N-1$). So the interesting case is where the system parameters are such that $\lambda = N$ lies within the window of instability. Then the steady state $(\mathbf{X}, A) = (\mathbf{X}^*, \mathbf{1})$ is unstable and thus state variable patterns will form, echoing the structure of (one or many of) the corresponding eigen-mode(s). This Turing driven symmetry loss may be exacerbated by the switch terms (depending upon the choice of ε being small enough), and then each sub-network will remain relatively well intra-connected, while becoming less well connected to the other sub-networks. Once relatively isolated, individuals within each of these sub-networks may evolve back towards the global equilibrium at $\mathbf{x}^*$, providing that $A(t)$ is such that the eigenvalues of Δ have by that time left the window of instability. Within such a less weightily connected network, all states will approach $\mathbf{x}^*$, the switch terms will become positive, and then the whole qualitative cycle can begin again.

Thus we expect aperiodic or pseudo-cyclic emergence and diminution of patterns, representing transient variations in attitudes in the form of different *norms* adopted by distinct sub-populations. As we shall see though, the trajectory of any individual may be sensitive and therefore effectively unpredictable, while the dynamics of the global behaviour is qualitatively predictable.

In the next section we introduce a specific case of the more general setting described here.

3. Examples

We wish to consider activator-inhibitor systems as candidates for the attitudinal dynamics in (1) and hence (3). The simplest such system has $M = 2$, with a single inhibitory variable, $x(t)$, and a single activational variable, $y(t)$. Let $\mathbf{x}_i(t) = (x_i(t), y_i(t))^T$ in (2), and consider the Schnackenberg dynamics [58, 59, 60] defined by the field

$$\mathbf{f}(\mathbf{x}_i) = (p - x_i y_i^2,\, q - y_i + x_i y_i^2)^T, \tag{6}$$

where $p > q \geq 0$ are constants. The equations have the required equilibrium point at

$$\mathbf{x}^* = \left(\frac{p}{(p+q)^2},\, p+q \right)^T, \tag{7}$$

and in order that $\mathbf{df}$ be a stability matrix, we must have

$$p - q < (p+q)^3.$$

We employ $\phi_{ij} = (x_i - x_j)^2$ as the homophily function and we must have $D = \mathrm{diag}(D_1, D_2)$ in (3).

When $M = 2$, the presence of Turing instability depends on the sign of the determinant of $(\mathbf{df}(\mathbf{x}^*) - D\lambda)$, which is quadratic in λ. For the Scnackenberg dynamics defined above, the roots of this quadratic are given by

$$\lambda_\pm = \frac{(p-q) - \frac{D_2}{D_1}(p+q)^3 \pm \sqrt{\left[(p-q) - \frac{D_2}{D_1}(p+q)^3\right]^2 - 4\frac{D_2}{D_1}(p+q)^4}}{2D_2(p+q)} > 0.$$

It is straightforward to show that if

$$\frac{D_2}{D_1} < \frac{3p + q - 2\sqrt{2p(p+q)}}{(p+q)^3} := \sigma_\mathrm{c}, \tag{8}$$

then $\lambda_\pm$ are real positive roots and hence $(\mathbf{df}(\mathbf{x}^*) - D\lambda)$ is a stability matrix if and only if λ lies outside of the interval (λ_-, λ_+), the *window of instability*. Inside there is always one positive and one negative eigenvalue, and the equilibrium $\mathbf{X}^*$ is unstable for any fixed network A. Note that, as is well known, it is the *ratio* of the diffusion constants that determines whether there is a window of instability.

3.1. Group dynamics

Now we present simulations of the Schnackenberg dynamics with $N = 10$. Parameter values are $p = 1.25$, $q = 0.1$, $\alpha = 10^4$, $\varepsilon = 10^{-6}$, $D_1 \approx 0.571$ and $D_2 \approx 0.037$. The ratio of the diffusion constants is $D_2/D_1 := \sigma = 0.9\sigma_\mathrm{c}$, and to ensure that the window of instability is centred on the fully coupled system we have

$$D_1 = \frac{(p-q) - \sigma(p+q)^3}{2\sigma N(p+q)}. \tag{9}$$

The initial coupling strengths were chosen uniformly at random between 0.1 and 0.5. The initial values of x and y were chosen at equally spaced intervals on a circle of radius 10^{-3} centred on the uniform equilibrium.

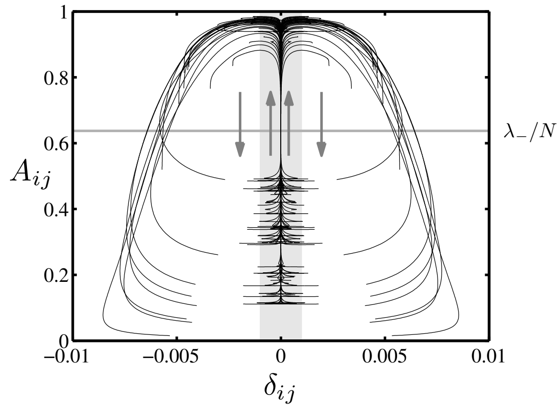

Figure 1: Trajectories of $\delta_{ij} := x_i - x_j$ and A_{ij} for all (i, j) pairs for unstable parameters integrated until $t \approx 440$. Parameter values and initial conditions are described in the main text. In the light grey shaded region, $\delta_{ij} < \varepsilon$ and the direction of trajectories are indicated with arrows. The grey horizontal line indicates the scaled stability threshold (unstable above, stable below).

In Figure 1 we illustrate the trajectories of $\delta_{ij} := x_i - x_j$ and the corresponding coupling strengths A_{ij} up to $t \approx 440$. The shaded region corresponds to $\delta_{ij} < \varepsilon$, within which the A_{ij} increase and outside of which they decrease, indicated by the dark grey arrows. The horizontal grey line marks the scaled instability threshold λ_-/N, which is indicative of the boundary of instability, above being unstable and below being stable. Because agents are only weakly coupled initially, their attitudes move towards the steady state $\mathbf{x}^*$, which causes the differences δ_{ij} to decrease. The switch terms subsequently become positive and hence the coupling strengths increase, along with the eigenvalues of the Laplacian λ_i. When one or more of the λ_i are within the window of instability, some of the differences δ_{ij} begin to diverge. However, this eventually causes their switch terms to become negative, reducing the corresponding coupling strengths and hence some of the λ_i. This then affects the differences δ_{ij}, which start to decrease, completing the qualitative cycle. As the system evolves beyond $t > 440$, this quasi-cyclic behaviour becomes increasingly erratic.

Although the long term behaviour of any given agent is unpredictable, the behaviour of the mean coupling strength of the system fluctuates around the instability boundary λ_-/N. In Figure 2(a), we plot the time series of the mean coupling strength, $\bar{A}(t) = \frac{1}{N(N-1)} \sum_{ij} A_{ij}$, between $t_1 = 5 \times 10^3$ and $t_2 = 10^4$. The dashed line indicates the instability boundary $\lambda_-/N \approx 0.6372$, which is very close to the time-averaged mean coupling strength $\langle A \rangle = \frac{1}{t_2 - t_1} \int_{t_1}^{t_2} \bar{A}(t)dt \approx 0.6343$. Also plotted in Figure 2 are snapshots of the network at six sequential times. To improve the visualisation of the network, the positions of nodes have been rotated by approximately 72°, since the differences in diffusion rates mean that the unrotated coordinates, (x, y), become contracted in one direction. The shading of the nodes corresponds to their average coupling strength and the shading of the edges correspond to their weight. In panel (b) the network is strongly coupled and node states are similar in the vertical direction, but less similar in the horizontal direction. In panels (c–e), two nodes disassociate from the group in opposite directions, which reduces the strength of their coupling to other nodes. In panel (f) the disassociated nodes start to move back towards the main group. This continues in panel (g), whilst two other nodes begin to disassociate from the group. This sequence illustrates the general scenario: agents' trajectories cycle around the origin with the network repeatedly contracting and expanding as agents become more and less similar in attitude respectively.

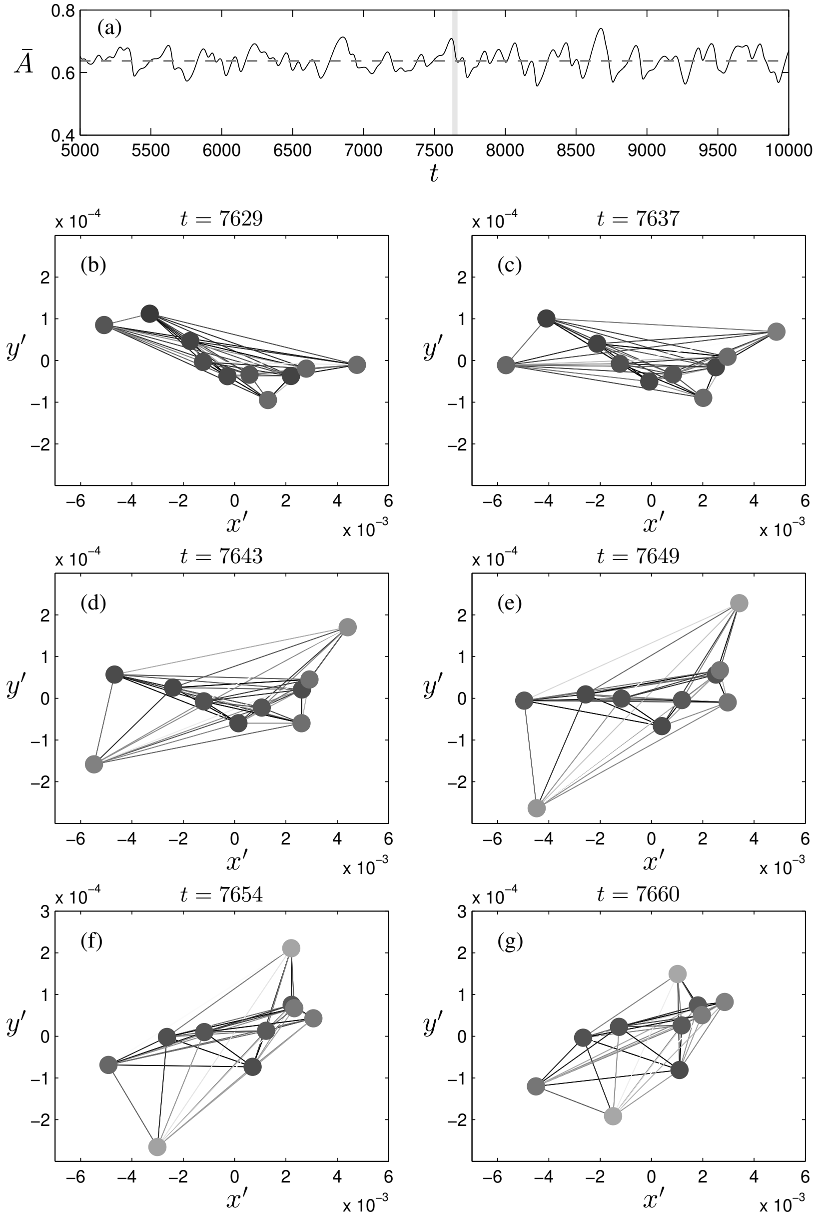

Figure 2: Panel (a): mean coupling strength, $\bar{A}(t)$, time series. Panels (b)–(g): network snapshots at sequential time intervals. Node positions are plotted in the rotated coordinates (x', y'), shading illustrates coupling strength for edges and mean coupling strength for nodes. Details of the dynamics are described in the main text.

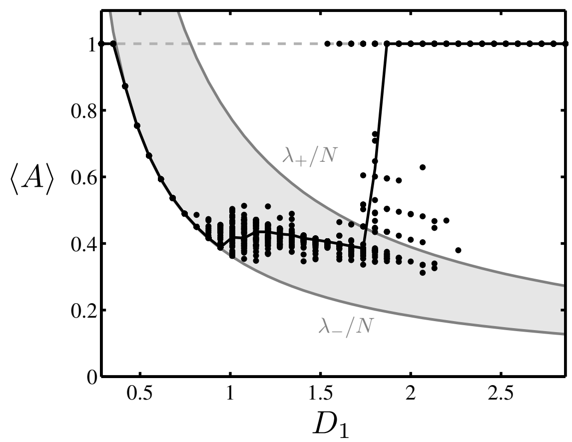

Figure 3: One parameter bifurcation diagram. The bifurcation parameter D_1 is plotted on the horizontal axis and the time averaged mean coupling strength $\langle A \rangle$ is plotted on the vertical axis. Black markers indicate corresponding values calculated from 50 realisations at each value of D_1. The black line corresponds to the median of the 50 realisations at each value of D_1. The dashed grey line indicates where $A = \mathbf{1}$. Shading indicates the scaled window of instability. Details of parameter values are described in the main text.

In Figure 3 we plot a one-parameter bifurcation diagram, based an ensemble of 2000 simulations whose initial conditions have been sampled at random using the method described in the example above. We use D_1 as a bifurcation parameter whilst keeping the ratio $D_2/D_1 = 0.9\sigma_{\mathrm{c}}$ held fixed. We simulate 50 realisations at 40 different values of D_1, with all remaining parameters held fixed at the values described above. We integrate each simulation until $t_2 = 1.5 \times 10^5$ and then compute the time-averaged mean coupling strength $\langle A \rangle$ from $t_1 = 1 \times 10^4$ to discount the effects of early transients. In Figure 3, at each value of D_1 we plot the value of $\langle A \rangle$ calculated for each realisation, indicated by black markers. The solid black line is the median of the 50 realisations at each value of D_1. The grey shaded region indicates the scaled window of instability, bounded by λ_+/N and λ_-/N. Thus the $A = \mathbf{1}$ equilibrium is unstable over an intermediate range of the D_1 values used. Figure 3 illustrates that at low values of D_1, all realisations equilibrate at $A = \mathbf{1}$. When the $A = \mathbf{1}$ equilibrium is unstable, the value of $\langle A \rangle$ calculated for all simulations follows the λ_-/N boundary closely. Interestingly, for a range of larger values of D_1 where the $A = \mathbf{1}$ equilibrium is stable, none of the realisations approach this equilibrium at large times. At larger values of D_1, all realisations once again reach the $A = \mathbf{1}$ equilibrium asymptotically. Thus, we have shown that when the $A = \mathbf{1}$ equilibrium is unstable, the average behaviour described by $\langle A \rangle$ is well approximated by λ_-/N and that this is not specific to a given set of parameters or initial conditions. In addition, for a range of values of D_1 the aperiodic dynamics have a significant basin of attraction, even when the $A = \mathbf{1}$ equilibrium is stable. We interpret this as evidence for the existence of a chaotic attractor.

3.2. Dyad dynamics

To probe the mechanism driving the aperiodic dynamics illustrated in Section 3.1, we consider a simpler dynamical setting consisting of just two agents. This reduces the coupling strength evolution (4) to a single equation, and hence five equations in total,

$$\dot{x}_1 = p - x_1 y_1^2 - D_1 a(x_1 - x_2), \tag{10}$$

$$\dot{x}_2 = p - x_2 y_2^2 + D_1 a(x_1 - x_2), \tag{11}$$

$$\dot{y}_1 = q - y_1 + x_1 y_1^2 - D_2 a(y_1 - y_2), \tag{12}$$

$$\dot{y}_2 = q - y_2 + x_2 y_2^2 + D_2 a(y_1 - y_2), \tag{13}$$

$$\dot{a} = \alpha a(1 - a) \left[\varepsilon - (x_1 - x_2)^2\right], \tag{14}$$

where $a(t) = A_{12}(t) = A_{21}(t)$ is the coupling strength.

In Figure 4, we plot the trajectories for each of the two agents (black and grey lines) in (x, y) space, and in (x, y, a) space in the upper-right inset. The parameter values are $p = 1.25$, $q = 0.1$, $\alpha = 10^4$, $\varepsilon = 10^{-6}$, $D_1 \approx 2.857$ and $D_2 \approx 0.184$. Again, the diffusion constants have the ratio $D_2/D_1 = 0.9\sigma_{\mathrm{c}}$ and the window of instability is centred on the fully coupled system via (9). The initial conditions are chosen near to the uniform equilibrium $\mathbf{x}^* = (x^*, y^*)^T$, specifically $x_1(0) = x^* + 1.5 \times 10^{-4}$, $x_2(0) = x^* - 1.5 \times 10^{-4}$, $y_1(0) = y^* - 1 \times 10^{-6}$, $y_2(0) = y^* + 1 \times 10^{-6}$; the initial coupling strength is $a(0) = 0.1$. This system is numerically stiff—on each cycle, trajectories get very close to the invariant manifolds $\mathbf{x} = \mathbf{x}^*$, $a = 0$ and $a = 1$—thus very low error tolerances are necessary in order to accurately resolve the trajectories.

The mechanisms driving the near cyclic behaviour illustrated in Figure 4 are qualitatively similar to those described in Section 2.1, but the present case is much simpler since the coupling constant, a, is a scalar. If we consider a as a parameter in the attitudinal dynamics (10–13), then Turing instability occurs as a pitchfork bifurcation at some $a = a_*$, where $0 < a_* < 1$ for our choice of parameters. The equilibria at $(\mathbf{x}, a) = (\mathbf{x}^*, 0)$ and $(\mathbf{x}^*, 1)$ are both saddle-foci, where the unstable manifolds are respectively parallel to the a-axis and entirely within the attitudinal state space, $\mathbf{x}$. Near to the $(\mathbf{x}^*, 1)$ equilibrium, a given trajectory tracks the unstable manifold of $(\mathbf{x}^*, 1)$ in one of two opposing directions, the choice of which is sensitively dependent on its earlier position when $a \approx a_*$. The combination of this sensitivity together with the spiral dynamics around the unstable manifold of $(\mathbf{x}^*, 0)$, leads to an orbit switching sides unpredictably on each near-pass of $(\mathbf{x}^*, 1)$ (c.f. the

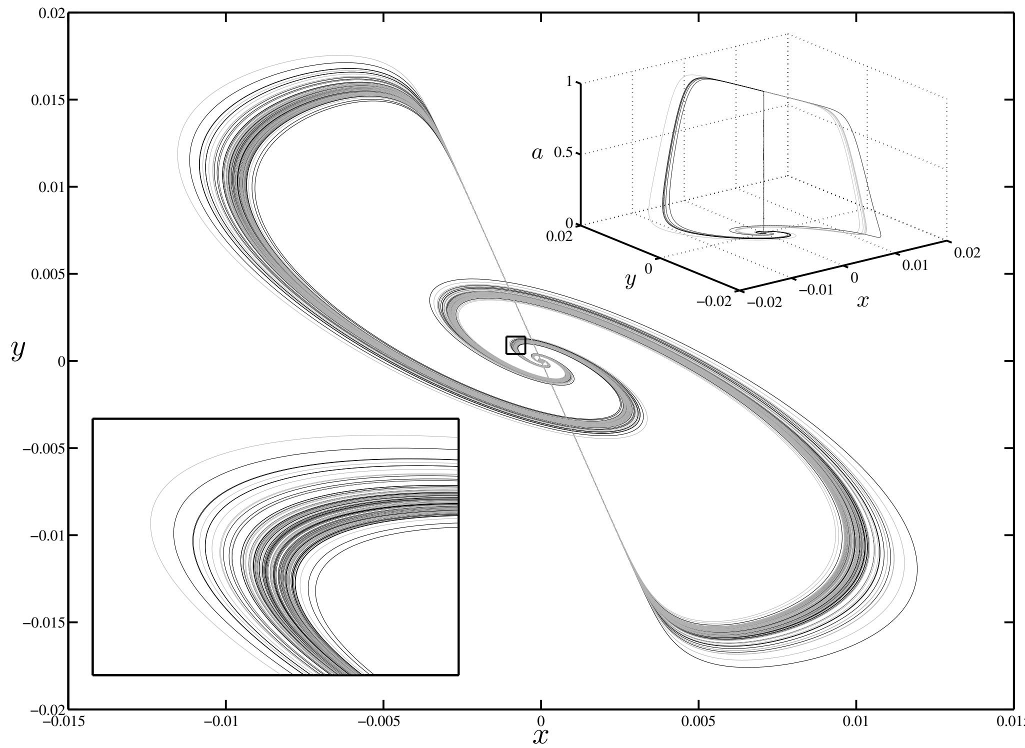

Figure 4: Main: Trajectories of dyadic system in (x, y) space with unstable parameters. Upper-right inset: Trajectories in (x, y, a) space. Lower-left inset: zoom of boxed region in the main plot. Parameters described in the main text.

top-right inset of Figure 4). The mechanism by which this chaotic behaviour arises is rather involved and warrants its own study, which we address in an article currently in preparation.

4. Summary and discussion

To summarise, we have proposed an adaptive network model to describe the evolution of sub-conscious attitudes within social groups. Our model incorporates social influence via diffusion and homophily via an evolving weighted network of coupling strengths. In addition, we have investigated whether node dynamics described by an activator-inhibitor process could give rise to polarisation of attitudes. While we have argued that such processes are natural in the context of *sub-conscious* attitude formation, the resulting dynamics illustrate that pattern formation mechanisms on adaptive networks prove to be interesting in their own right. While we do not observe stationary polarised states, in certain parameter regimes we do see aperiodic temporal patterns, corresponding to convergence and divergence of attitudinal states and, respectively, strengthening and weakening of the coupling network.

Now we discuss our model in the context of other models of attitudinal dynamics and ‘cultural’ (meaning any attribute subject to social influence) polarisation [47, 12, 48]. Interest in such models largely stems from the work of Axelrod [47], who demonstrated that local convergence could lead to cultural polarisation. However, such states typically do not persist when there is noise, representing cultural drift [52][2]. This does not seem surprising, since in the absence of noise, the mechanisms employed by such cultural

[2]Polarised states that occur when the network becomes disconnected [11, 13, 16] may

dissemination models typically *reduce* diversity. However, an approach that allows diversity to increase via xenophobia has been suggested by Flache and Macy [48]. The effects of cultural drift have not been investigated in this model but monoculture is still an absorbing state.

In the model presented in this paper, diversity can increase as a consequence of Turing instability. Furthermore, we can identify regions in which global monoculture is *unstable*. For a fixed network, where A does not evolve, this instability arises from a pitchfork bifurcation, which gives rise to stable 'Turing patterns' [61], where nodes adopt either of two stable states. Nodes in these two stable states must necessarily have connections between them for (2) to be in equilibrium. When the network is allowed to evolve, as in our model, such states can only be stable if the network evolution equations also reach a non-trivial stable equilibrium, meaning that all switch terms are zero. However, we have seen no evidence of this occurring in numerical simulations. Thus in its present form, sub-group formation and polarisation appear to be transient phenomena in our model. Extensions to our model, e.g. including heterogeneous agent behaviour, could however result in stable polarised equilibria.

Our model, based on a deterministic dynamical system, has allowed us to use standard stability analysis techniques to analyse consensus equilibria and map out parameter regimes that give rise to aperiodic dynamics. Moreover, dynamical regimes and bifurcation phenomena may also be investigated using numerical continuation, which we will address in future work. But in-

also be unstable when edges are occasionally rewired at random.

terestingly, even though our model is deterministic and at the system level its dynamics are qualitatively predictable (sub-group formation and dissolution whose average behaviour centres on the boundary of instability[3]), it still gives rise to dynamics that at the level of individual agent journeys are chaotic and entirely unpredictable. While somewhat of a leap, this raises an interesting question: are the mechanisms that govern our behaviour the cause of its volatility? We believe that studying simple mathematical models, such as ours, may provide valuable insights into collective human behaviour as well as interesting mathematics.

Acknowledgements

JAW and PG acknowledge the EPSRC for support through MOLTEN (EP/I016058/1). We would like to thank Jon Dawes, Michael Macy and those at the Centre for Mathematics of Human Behaviour for their valuable input, discussion and comments.

References

[1] T. Gross, B. Blasius, Adaptive coevolutionary networks: a review, J. R. Soc. Interface 5 (2007) 259–271.

[2] J. Ito, K. Kaneko, Spontaneous structure formation in a network of dynamic elements, Phys. Rev. E 67 (2003) 046226.

[3] A stochastic model based on similar principles to those described in this paper is presented in [62], where qualitatively similar dynamical phenomena are also observed.

[3] C. Zhou, J. Kurths, Dynamical weights and enhanced synchronization in adaptive complex networks, Phys. Rev. Lett. 96 (2006) 164102.

[4] A. Arenas, A. Diaz-Guilera, J. Kurths, Y. Moreno, C. Zhou, Synchronization in complex networks, Phys. Rep. 469 (2008) 93–153.

[5] T. Gross, C. J. Dommar DLima, B. Blasius, Epidemic dynamics on an adaptive network, Phys. Rev. Lett. 96 (2006) 208701.

[6] T. Gross, I. G. Kevrekidis, Robust oscillations in SIS epidemics on adaptive networks: Coarse graining by automated moment closure, Europhys. Lett. 82 (2008) 38004.

[7] H. Ebel, S. Bornholdt, Coevolutionary games on networks, Phys. Rev. E 66 (2002) 056118.

[8] M. G. Zimmermann, V. M. Eguíluz, Cooperation, social networks, and the emergence of leadership in a prisoners dilemma with adaptive local interactions, Phys. Rev. E 72 (2005) 056118.

[9] J. M. Pacheco, A. Traulsen, M. A. Nowak, Coevolution of strategy and structure in complex networks with dynamical linking, Phys. Rev. Lett. 97 (2006) 258103.

[10] P. Holme, M. E. J. Newman, Nonequilibrium phase transition in the coevolution of networks and opinions, Phys. Rev. E 74 (2006) 1–5.

[11] S. Gil, D. H. Zanette, Coevolution of agents and networks: Opinion spreading and community disconnection, Phys. Lett. A 356 (2006) 89–94.

[12] D. Centola, J. C. González-Avella, V. M. Eguíluz, M. San Miguel, Homophily, cultural drift, and the co-evolution of cultural groups, J. Conflict Resolut. 51 (2007) 905–929.

[13] B. Kozma, A. Barrat, Consensus formation on adaptive networks, Phys. Rev. E 77 (2008) 1–10.

[14] J. Bryden, S. Funk, N. Geard, S. Bullock, V. A. Jansen, Stability in flux: community structure in dynamic networks, J. R. Soc. Interface 8 (2011) 1031–1040.

[15] M. Mobilia, Fixation and polarization in a three-species opinion dynamics model, Europhys. Lett. 95 (2011) 1–6.

[16] R. Durrett, J. P. Gleeson, A. L. Lloyd, P. J. Mucha, F. Shi, D. Sivakoff, J. E. S. Socolar, C. Varghese, Graph fission in an evolving voter model, Proc. Natl. Acad. Sci. USA 109 (2011) 3683–3687.

[17] P. De Lellis, M. di Bernardo, F. Garofalo, Synchronization of complex networks through local adaptive coupling, Chaos 18 (2008) 037110.

[18] J. Rodriguez, M.-O. Hongler, Networks of self-adaptive dynamical systems, IMA J. Appl. Math. 79 (2014) 201–240.

[19] N. E. Friedkin, E. C. Johnsen, Social influence networks and opinion change, Advances in Group Processes 16 (1999) 1–29.

[20] R. Hegselmann, U. Krause, Opinion dynamics and bounded confidence models, analysis, and simulation, JASSS–J. Artif. Soc. S. 5 (2002).

[21] C. Castellano, S. Fortunato, V. Loreto, Statistical physics of social dynamics, Rev. Mod. Phys. 81 (2009) 591–646.

[22] M. Sherif, The Psychology of Social Norms, Harper, Oxford, England, 1936.

[23] S. E. Asch, Effects of group pressure upon the modification and distortion of judgment, in: Groups, Leadership and Men, Carnegie Press, Pittsburgh, USA, 1951.

[24] D. T. Campbell, Conformity in psychology's theories of acquired behavioural disposition, in: Conformity and Deviation, Harper, New York, USA, 1963.

[25] S. Milgram, Liberating effects of group pressure, J. Pers. Soc. Psychol. 1 (1965) 127–134.

[26] B. E. Collins, R. D. Ashmore, Social Psychology: Social Influence, attitude change, group processes and prejudice, Addison-Wesley, Reading, USA, 1970.

[27] M. McPherson, L. Smith-Lovin, J. M. Cook, Birds of a feather: Homophily in social networks, Ann. Rev. Soc. 27 (2001) 415–444.

[28] T. W. Valente, Social network thresholds in the diffusion of innovations, Soc. Networks 18 (1996) 69–89.

[29] D. J. Watts, A simple model for global cascades on random networks, Proc. Natl. Acad. Sci. USA 99 (2002) 5766–5771.

[30] L. M. A. Bettencourt, A. Cintron-Arias, D. I. Kaiser, C. Castillo-Chavez, The power of a good idea: Quantitative modeling of the spread of ideas from epidemiological models, Physica A 364 (2006) 513–536.

[31] J. Onnela, F. Reed-Tsochas, Spontaneous emergence of social influence in online systems, Proc. Natl. Acad. Sci. USA 107 (2010) 18375–18380.

[32] P. L. Krapivsky, S. Redner, D. Volovik, Reinforcement-driven spread of innovations and fads, J. Stat. Mech.-Theory E. 12 (2011) 1–12.

[33] P. S. Dodds, D. J. Watts, A generalized model of social and biological contagion, J. Theor. Biol. 232 (2005) 587–604.

[34] D. Centola, V. M. Eguiluz, M. W. Macy, Cascade dynamics of complex propagation, Physica A 374 (2007) 449–456.

[35] D. Lopez-Pintado, D. J. Watts, Social influence, binary decisions and collective dynamics, Ration. Soc. 20 (2008) 399–443.

[36] S. Melnik, J. A. Ward, J. P. Gleeson, M. A. Porter, Multi-stage complex contagions, Chaos 23 (2013) 013124.

[37] M. Granovetter, Threshold models of collective behavior, Am. J. Sociol. 83 (1978) 1420–1443.

[38] J. H. Fowler, N. A. Christakis, Cooperative behavior cascades in human social networks, Proc. Natl. Acad. Sci. USA 107 (2010) 5334–5338.

[39] D. Baldassarri, P. Bearmann, Dynamics of political polarization, Am. Sociol. Rev. 72 (2007) 784–811.

[40] E. Ben-Naim, P. L. Krapivsky, F. Vazquez, S. Redner, Unity and discord in opinion dynamics, Physica A 330 (2003) 99–106.

[41] N. J. McCullen, M. V. Ivanchenko, V. D. Shalfeev, W. F. Gale, A dynamical model of decision-making behaviour in a network of consumers with applications to energy choices, Int. J. Bif. Chaos 21 (2011) 2467–2480.

[42] Y. Shoham, M. Tennenholtz, On the emergence of social conventions: modeling, analysis, and simulations, Artif. Intell. 94 (1997) 139–166.

[43] N. E. Friedkin, Norm formation in social influence networks, Soc. Networks 23 (2001) 167–189.

[44] D. Centola, R. Willer, M. M., The emperors dilemma: A computational model of self-enforcing norms, Am. J. Sociol. 110 (2005) 1009–1040.

[45] K. Carley, A theory of group stability, Am. Sociol. Rev. 56 (1991) 331–354.

[46] N. Mark, Beyond individual differences: Social differentiation from first principles, Am. Sociol. Rev. 63 (1998) 309–330.

[47] R. Axelrod, The dissemination of culture, J. Conflict Resolut. 41 (1997) 203–226.

[48] A. Flache, M. W. Macy, Small worlds and cultural polarization, J. Math. Soc. 35 (2011) 146–176.

[49] S. Aral, L. Muchnik, A. Sundararajan, Distinguishing influence-based contagion from homophily-driven diffusion in dynamic networks, Proc. Natl. Acad. Sci. USA 106 (2009) 21544–21549.

[50] C. R. Shalizi, A. C. Thomas, Homophily and contagion are generically confounded in observational social network studies, Sociol. Method Res. 40 (2011) 211–239.

[51] M. W. Macy, J. A. Kitts, A. Flache, S. Benard, Polarization in dynamic networks: A Hopfield model of emergent structure, in: Dynamic Social Network Modeling and Analysis, The National Acadamy Press, Washington D.C., USA, 2003.

[52] K. Klemm, E. V. M., R. Toral, M. San Miguel, Globalization, polarization and cultural drift, J Econ. Dyn. Control 29 (2005) 321–334.

[53] P. J. Morgane, J. R. Galler, D. J. Mokler, A review of systems and networks of the limbic forebrain/limbic midbrain, Prog. Neurobiol. 75 (2005) 143–160.

[54] G. Mathews, K. Gilliland, The personality theories of H. J. Eysenck and J. A. Gray: a comparative review, Pers. Indiv. Differ. 26 (1999) 583–626.

[55] H. J. Eysenck, The biological basis of personality, Thomas, Springfield, USA, 1967.

[56] J. A. Gray, The psychology of fear and stress, Cambridge University Press, UK, Cambridge, 2nd edition, 1987.

[57] J. A. Bargh, T. L. Chartrand, The unbearable automaticity of being, Am. psychol. 54 (1999) 462.

[58] J. Murray, Mathematical Biology: I. An Introduction, Interdisciplinary Applied Mathematics, Springer-Verlag, New York, USA, 2002.

[59] J. Murray, Mathematical Biology II: Spatial Models and Biomedical Applications, Interdisciplinary Applied Mathematics: Mathematical Biology, Springer-Verlag, New York, USA, 2003.

[60] P. Grindrod, The Theory and Applications of Reaction-diffusion Equations: Patterns and Waves, Oxford applied mathematics and computing science series, Clarendon Press, 2nd edition, 1996.

[61] H. Nakao, A. S. Mihailov, Turing patterns in network-organized activatorinhibitor systems, Nat. Phys. 6 (2010) 544–550.

[62] P. Grindrod, M. Parsons, Complex dynamics in a model of social norms, 2012. Unpublished.